SMAR 2015 – Third Conference on Smart Monitoring,
Assessment and Rehabilitation of Civil Structures

SMAR 2015

Plastic hinge length and ultimate drift of FRP-confined circular columns under seismic loading

Osama Youssf [1], Mohamed A. ElGawady[2], and Julie E. Mills[3]

[1] PhD student, University of South Australia, Adelaide, Australia.
[2] Associate Professor, Missouri University of Science and Technology, Rolla, USA.
[3] Professor and head of school of NBE, University of South Australia, Adelaide, Australia.

ABSTRACT: This paper presents a finite element (FE) model that was developed using the LS-DYNA program aimed at modelling the plastic hinge length (l_p) and ultimate drift ratio (δ_u) for FRP-confined RC columns. A FE parametric study was conducted to investigate the effect of FRP-confinement on l_p. Empirical models were proposed to predict l_p and δ_u for FRP-confined RC columns and the results were compared with similar previous models. The proposed FE model was able to predict the plastic hinge region and l_p value which can provide a simple way for designers to investigate the behaviour of FRP-confined columns during the design process. The proposed δ_u model reduced the mean error (M) and standard deviation (SD) by 34.8%, 46.3%, respectively, compared to the best predictions by previous models.

1 INTRODUCTION

In recent years, external confinement of concrete columns by fibre reinforced polymer (FRP) has become increasingly popular in the construction industry. FRP-confinement increases the column's shear resistance and ductility because of its high tensile stiffness and strength. FRP-confinement prevents concrete cover from spalling and increases the inelastic deformability of concrete in the potential plastic hinge region, which can increase the lateral displacement capacity of the column under seismic loads (Ozbakkaloglu and Saatcioglu 2007). Therefore, using FRP to confine concrete columns subject to seismic loads is an important design or rehabilitation option to consider.

The plastic hinge region is defined as the physical region over which the member experiences inelastic deformations and severe damage (Ozbakkaloglu and Idris 2014). The performance of a plastic hinge is critical to the deformation capacities of flexural members and hence requires extensive detailing to prevent failure of structural members from extreme events such as earthquakes. Identification of the plastic hinge length (l_p) is a key step in estimating the ultimate drift ratio (δ_u) of concrete columns. Priestley et al. (1996) and Elsanadedy and Haroun (2005) showed that l_p of an FRP-confined RC column is smaller than that of a traditional RC column. However, other experimental tests have also shown that the l_p of FRP-confined columns are larger than those of traditional RC columns (Ozbakkaloglu and Saatcioglu 2006). Other researchers reported that the l_p of FRP-confined columns is equal to that of a traditional RC columns (Binici 2008). Hence, there is no consensus among researchers on the quantification of l_p for FRP-confined columns. Therefore, quantification of the plastic hinge zone is important,

not only for the design of new structures but also for the rehabilitation of old structures (Zhao, Wu and Leung 2012).

Several analytical models have been developed for estimating l_p for unconfined columns. These models resulted in a wide range of l_p values ranging from 0.4 to 2.4 of the column's diameter. However, limited studies were conducted to determine l_p for FRP-confined columns (Gu, Wu, Wu et al. 2012). By estimating l_p for a given column, δ_u can be estimated due to the good correlation between them (Paulay and Priestly 1992; Gu et al. 2012). In the current research, finite element (FE) models developed using LS-DYNA were used to investigate the plastic hinge length in different FRP-confined RC columns. Six FRP-confined RC columns were used to calibrate the proposed FE model. A parametric study was conducted using the developed FE model to investigate the effect of confinement on l_p. Then, based on the FE results, empirical models were proposed to determine the values of l_p and δ_u of FRP-confined columns. The proposed δ_u model predictions were compared to the predictions of two previous models.

2 FINITE ELEMENT MODELING

The concrete footing, column, and loading stub in this study were modelled using 8-node constant stress solid hexahedron elements. FRP jackets were modelled using 4-node shell elements. The reinforcement bars were modelled using 2-node beam elements. The column was laterally loaded in displacement control uniformly applied to all nodes at the mid-height of the column loading stub. The axial load on the column was applied on the top surface of the column loading stub. The K-C model, *MAT_CONCRETE_DAMAGE_RELIII, was used for simulating the concrete material for the columns (Malvar, Crawford and Morrill 2000). It was used in conjunction with an equation of state, EOS_TABULATED_COMPACTION, which gives the current pressure, P, as a function of current and previous volumetric strain. By knowing the compressive strength of the column under modelling, the material model parameters were automatically generated using a standard 100x200 mm cylinder and then these parameters were implemented in the full scale model. However, parameter b1 was calibrated based on the full scale model and a value of 2.5 was used. More details and features of this material model can be found in (Simons 1995; Malvar, Crawford, Wesevich et al. 1996). The FRP Jacket was modelled using an orthotropic material model called MAT_ORTHOTROPIC_ ELASTIC_002 material model (LS-DYNA Keyword User's Manual 2007). The MAT_ADD_ EROSION card was used to control the failure stress of the FRP shell. The contact between the FRP jacket and the concrete column was assumed as a perfect bond by sharing the same nodes at the contact surface, as recommended by previous FE studies, e.g. (Elsanadedy, Al-Salloum, Alsayed et al. 2012; Mohammed 2012; Youssf, ElGawady, Mills et al. 2014). The reinforcement bars were modelled using an elastoplastic material model (MAT_PLASTIC_ KINEMATIC_003). The reinforcement was modelled using a discrete representation with perfect bond between any reinforcement bars and the concrete.

3 EXPERIMENTAL DATABASE

A total of 39 circular FRP-confined RC columns were collected from the literature as an experimental database in this study, see Table 1. In this table, D is the specimen diameter, H is the specimen shear span, f'_c is the unconfined concrete compressive strength, P is the column axial load, P_0 is the column axial load capacity calculated using Equation 1 according to (ACI-318 2011), t_f is the saturated FRP thickness, and f_t is the FRP ultimate tensile strength.

$$P_0 = 0.85\left(A_g - A_s\right) f_c' + A_s\, f_{sy} \quad (1)$$

where, A_g is the gross area of column cross section, A_s is the total area of longitudinal reinforcement, f_c' is the unconfined concrete compressive strength, and f_{sy} is the yeild strength of the longitudinal reinforcement.

4 VALIDATION OF THE PROPOSED FE MODEL

The first six specimens of the database shown in Table 1 were used to calibrate the proposed FE model. The calibration was carried out by comparing the predicted backbone curves with the corresponding experimental ones. Figure 1 shows examples of the FE model backbone curve predictions compared to the corresponding experimental ones. As shown in the figure, the FE models were able to capture the elastic and plastic behaviour of the column specimens quite well.

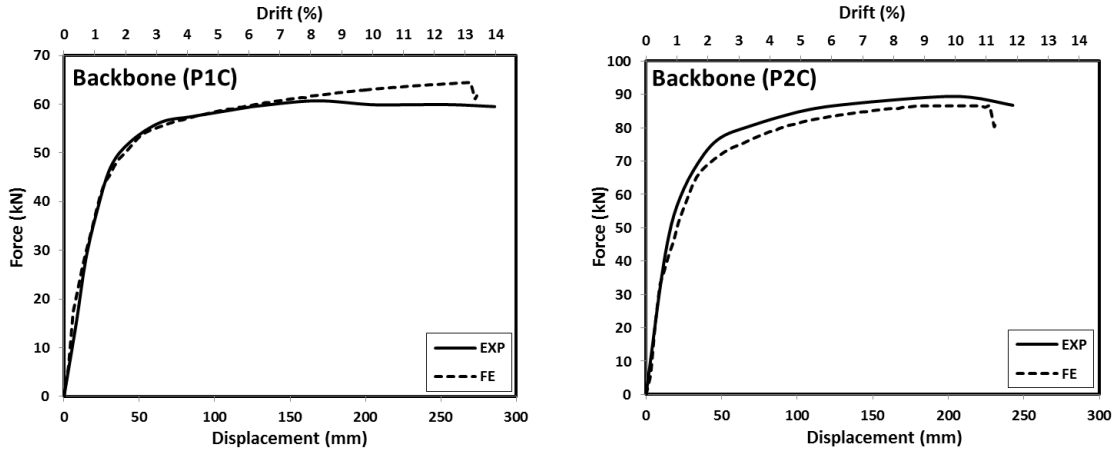

Figure 1. Experimental versus FE backbone curve predictions.

5 MODELLING OF THE PLASTIC HINGE LENGTH

Based on the FE model results, l_p was measured using the technique previously proposed and verified by (Ozbakkaloglu and Saatcioglu 2006; Ozbakkaloglu and Saatcioglu 2007; Idris and Ozbakkaloglu 2013; Ozbakkaloglu and Idris 2014) and reported for each specimen. In order to do that, the hoop strain experienced at each level of the column height was recorded at each column's ultimate displacement. Then the hoop-strain profile along the column height was used to determine l_p as the height above the column footing where the recorded hoop strain values were below 1/3 of the maximum recorded strain.

A parametric study was conducted on the six specimens in Table 1 to better understand the effect of the FRP-confinement on l_p using the above described FE model by running each model eight times with different values of λ_l. The confinement ratio $\left[\lambda_l = \frac{2\, f_t\, t_f}{D\, f_c'}\right]$ of each column was changed by changing the confinement thickness, t_f. ACI 440-2R (2008) recommended that the confinement ratio should be larger than 0.08. Moreover, in practice,

achieving a passive confinement ratio as large as 0.70 is quite difficult considering the large size of real concrete columns and the cost of confinement materials (Yazici and Hadi 2012). In previous experimental studies, the confinement ratio usually ranged between 0.10 and 0.50. Therefore, the chosen confinement ratio limits in this parametric study ranged between 0.08 and 0.70 to cover the recommended ranges.

Table 1. Experimental database of FRP-confined RC columns.

No.	ID	D (mm)	H (mm)	f'_c (MPa)	P/P_0 (%)	FRP type	t_f (mm)	f_t (MPa)	Source
1	P1C	300	2045	35.8	8	C	1.02	849	(Desprez, Mazars, Kotronis et al. 2013)
2	P2C	300	2045	34.9	31	C	1.02	849	(Desprez et al. 2013)
3	P3C	300	2045	34.4	9	C	1.02	849	(Desprez et al. 2013)
4	P4C	300	2045	34.3	29	C	1.02	849	(Desprez et al. 2013)
5	RC2	270	2000	75.2	34	C	0.33	3800	(Ozbakkaloglu and Saatcioglu 2006)
6	RC3	270	2000	49.7	47	C	0.33	3800	(Ozbakkaloglu and Saatcioglu 2006)
7	RC1	270	2000	90.1	31	C	0.66	3800	(Ozbakkaloglu and Saatcioglu 2006)
8	RC4	270	1200	75.3	34	C	0.33	3800	(Ozbakkaloglu and Saatcioglu 2006)
9	CFFT	150	1000	95.0	41	A	0.60	2900	(Idris and Ozbakkaloglu 2013)
10	S2	300	750	31.3	31	C	0.17	3710	(Zhou, Lu, Li et al. 2013)
11	S17	300	750	31.3	31	C	0.17	3710	(Zhou et al. 2013)
12	FCS-1	760	1750	18.6	4	C	0.41	4170	(Li and Sung 2004)
13	FCS-2	760	1750	18.6	4	C	0.28	4170	(Li and Sung 2004)
14	CH1	360	1100	34.9	24	C + D	0.34	2346	(Gu, Wu, Wu et al. 2010)
15	CH3	360	1100	34.9	24	C	0.25	3945	(Gu et al. 2010)
16	J1	300	850	28.0	3	D	0.26	1832	(Gu et al. 2010)
17	J2	300	850	28.0	3	C	0.11	4232	(Gu et al. 2010)
18	J3	300	850	28.0	3	C	0.11	4232	(Gu et al. 2010)
19	CL1	360	800	34.9	24	D	1.03	1832	(Gu et al. 2010)
20	CL2	360	800	34.9	24	C	0.42	3945	(Gu et al. 2010)
21	ST-2NT	356	1470	40.4	54	G	1.25	828	(Sheikh and Yau 2002)
22	ST-3NT	356	1470	40.4	55	C	1.00	805	(Sheikh and Yau 2002)
23	ST-4NT	356	1470	44.8	27	C	0.50	1675	(Sheikh and Yau 2002)
24	CCF2	240	1500	62.5	4	C	0.26	4300	(Youssf, ElGawady and Mills 2015)
25	CRCF2	240	1500	46.4	5	C	0.26	4300	(Youssf et al. 2015)
26	CS-ISJ-RT	610	915	35.9	6	G	10.16	552	(Xiao, Wu and Martin 1999)
27	CS-CSJ-RT	610	915	35.9	6	G	7.62	552	(Xiao et al. 1999)
28	J4	300	850	28.0	3	D	0.516	1832	(Gu et al. 2010)
29	J5	300	850	28.0	3	C	0.222	4232	(Gu et al. 2010)
30	J6	300	850	28.0	3	C + D	0.369	2552	(Gu et al. 2010)
31	J7	300	850	28.0	3	C + D	0.3135	2255	(Gu et al. 2010)
32	CH2	360	1100	34.9	24	D	0.65	1832	(Gu et al. 2010)
33	CL3	360	800	34.9	24	C	0.58	3945	(Gu et al. 2010)
34	C1n1	180	630	54.8	45	C	0.80	3430	(Wang, Wang, Sheikh et al. 2011)
35	C1n2	180	630	54.8	55	C	0.80	3430	(Wang et al. 2011)
36	C1n3	180	630	54.8	65	C	0.80	3430	(Wang et al. 2011)
37	C2n1	180	630	71.2	47	C	0.80	3430	(Wang et al. 2011)
38	C2n2	180	630	71.2	57	C	0.80	3430	(Wang et al. 2011)
39	C2n3	180	630	71.2	68	C	0.80	3430	(Wang et al. 2011)

C	Carbon fiber	A	Aramid fiber
G	Glass fiber	D	Dyneema fiber

Figure 2 shows the results of the parametric study. Generally, increasing the confinement ratio increases the plastic hinge length. Up to a confinement ratio of 0.4 the rate of increase in l_p is relatively higher than the rate of increase beyond a confinement ratio of 0.4. The decreased significance of the FRP-confinement at high λ_l can be attributed to the column failure mode. At relatively low confinement ratios the column's failure was mainly due to rupture of the FRP. However, at relatively high confinement ratios the column's failure was mainly due to rupture of the longitudinal reinforcement rather than rupture of the FRP, thus reducing the significance of the FRP-confinement.

The plastic hinge lengths measured from the FE models for the original six calibrated specimens and the parametric study resulted in a total of fifty four l_p values. Previous published plastic hinge models were used in this study to find the model that best fit the results of these fifty four l_p values. Through investigating the mean error (M) and standard deviations (SD) in the predictions of those previous models, the Paulay and Priestly (1992) model (Equation 2) gave the lowest M and SD compared to other previous models. In this study, Equation 2 was modified to take into consideration the effect of the FRP-confinement and hence generate better l_p predictions for FRP-confined columns, with lower M and SD. The final form of the modified l_p model is shown in Equation 3. The M and SD of the proposed l_p model were 23.6% and 16.9%, respectively, compared to the M and SD of 44.5% and 16.6%, respectively of the Paulay and Priestly (1992) model predictions, through the fifty four l_p values. Thus, the proposed l_p model reduced the M by 47% compared to the earlier model, however, the SD slightly increased by 1.8%. The proposed l_p model will be used in developing the prediction of the ultimate drift ratio of FRP-confined columns in next section.

$$l_p = 0.08\,H + 0.022\,f_{sy}\,d_b \tag{2}$$

$$l_p = 0.6\,\lambda_l\,H + 0.022\,f_{sy}\,d_b \tag{3}$$

where, l_p is the plastic hinge of FRP-confined column, H is the column shear span, λ_l is the confinement ratio, f_{sy} is the rebar yield strength, and d_b is the longitudinal rebar diameter.

6 MODELLING OF THE ULTIMATE DRIFT RATIO

In order to model the column ultimate drift ratio (δ_u), two previous models namely, Paulay and Priestly (1992) model and Gu et al. (2012) model were used to predict the results of the collected database as shown in Table 2.

As shown in Table 2, the Gu et al. (2012) model was able to predict δ_u with M of 51.7% less than the M of Paulay and Priestly (1992) predictions using their own l_p models. Thus, it was decided in this study to modify the Gu et al. (2012) model that shown in Equation 4 to achieve better predictions of δ_u. The final modified model, Equation 5, predictions were compared with previous models through the whole 39 specimens in the database as shown in Table 2.

$$\delta_u = \frac{2.45\,\varepsilon_{sy}\,H}{3\,D} + \left[\frac{0.008+0.09\,\lambda_l}{0.19+\left(\frac{P}{P_0}\right)(0.72-0.67\,\lambda_l)} - 2.45\,\varepsilon_{sy}\right]\left(\frac{l_p}{H}\right)\left(1-0.5\,\frac{l_p}{H}\right)\left(\frac{H}{D}\right) \tag{4}$$

Table 2. Predicted δ_u values using different models.

No.	ID	EXP.	Paulay and Priestly (1992)		Gu et al. (2012)		Proposed model (Eq. 5)	
		δu	δu	Error (%)	δu	Error (%)	δu	Error (%)
1	P1C	0.140	0.098	30.1	0.194	38.5	0.122	13.0
2	P2C	0.119	0.054	54.5	0.122	3.3	0.078	34.6
3	P3C	0.140	0.113	18.8	0.189	35.5	0.122	12.8
4	P4C	0.073	0.078	5.9	0.127	73.0	0.081	10.6
5	RC2	0.100	0.020	79.5	0.117	17.3	0.066	33.5
6	RC3	0.091	0.019	78.6	0.110	21.3	0.077	15.6
7	RC1	0.121	0.023	80.7	0.139	14.8	0.103	14.9
8	RC4	0.040	0.013	68.7	0.076	89.3	0.050	24.3
9	CFFT	0.103	0.020	80.8	0.124	20.1	0.110	6.3
10	S2	0.032	0.018	43.3	0.053	67.7	0.041	28.8
11	S17	0.035	0.018	48.9	0.053	51.4	0.041	16.2
12	FCS-1	0.068	0.018	73.6	0.076	12.6	0.071	5.1
13	FCS-2	0.058	0.018	69.0	0.075	29.5	0.049	14.9
14	CH1	0.050	0.017	66.2	0.066	32.4	0.046	8.6
15	CH3	0.080	0.017	78.9	0.072	10.1	0.052	34.9
16	J1	0.085	0.030	64.2	0.096	13.5	0.067	20.9
17	J2	0.086	0.030	64.6	0.096	11.9	0.067	22.1
18	J3	0.086	0.030	64.6	0.096	11.9	0.067	22.1
19	CL1	0.068	0.014	79.1	0.074	9.3	0.072	6.6
20	CL2	0.060	0.014	76.4	0.071	17.8	0.064	7.5
21	ST-2NT	0.046	0.021	53.4	0.060	31.2	0.045	1.8
22	ST-3NT	0.046	0.021	53.4	0.053	15.1	0.039	15.1
23	ST-4NT	0.080	0.027	65.7	0.078	2.4	0.054	32.1
24	CCF2	0.097	0.139	43.6	0.197	102.7	0.123	26.7
25	CRCF2	0.098	0.150	52.8	0.199	103.2	0.152	55.0
26	CS-ISJ-RT	0.125	0.011	91.2	0.053	57.4	0.107	14.5
27	CS-CSJ-RT	0.173	0.011	93.6	0.049	71.7	0.077	55.8
28	J4	0.126	0.030	75.9	0.119	5.5	0.108	14.4
29	J5	0.112	0.030	72.8	0.119	6.2	0.107	4.2
30	J6	0.125	0.030	75.7	0.119	4.8	0.108	14.0
31	J7	0.109	0.030	72.1	0.111	1.5	0.086	20.8
32	CH2	0.130	0.017	87.0	0.077	41.1	0.059	54.7
33	CL3	0.060	0.014	76.3	0.080	33.7	0.087	44.9
34	C1n1	0.114	0.012	89.4	0.091	20.2	0.131	14.5
35	C1n2	0.116	0.011	91.0	0.083	28.4	0.116	0.7
36	C1n3	0.126	0.002	98.1	0.077	39.2	0.103	17.9
37	C2n1	0.136	0.002	98.3	0.068	50.2	0.094	31.0
38	C2n2	0.133	0.002	98.2	0.061	54.1	0.083	37.8
39	C2n3	0.137	0.002	98.3	0.056	59.4	0.074	46.0
	M (%)			69.6		33.6		21.9
	SD (%)			21.1		27.4		14.7
	Max. error (%)			98.3		103.2		55.8

$$\delta_u = \frac{2.25\,\varepsilon_{sy}\,H}{3\,D} + \left[\frac{0.01+0.05\,\lambda_l}{0.17+\left(\frac{P}{P_0}\right)(0.7-0.1\,\lambda_l)}\right]\left(\frac{1.2\,l_p}{D}\right)\left(1-0.5\,\frac{l_p}{H}\right) \quad (5)$$

where, δ_u is the ultimate drift ratio of the FRP-confined column, ε_{sy} is the yield strain of the longitudinal reinforcement, H is the specimen shear span, D is the specimen diameter, λ_l is the

confinement ratio, P is the axial load, P_0 is the column axial load capacity, and l_p is the plastic hinge length of the FRP-confined column.

From Table 2 and compared to the experimental results, the M, SD, and max. error were 21.9% 14.7%, and 55.8%, respectively in the proposed δ_u model predictions, 33.6%, 27.4%, and 103.2%, respectively in the Gu et al. model prediction, and 69.6%, 21.1%, and 98.3%, respectively in the Paulay and Priestly model predictions, as shown in Figure 3. Thus, the proposed model significantly decreased M, SD, and max. error by 34.8%, 46.3%, and 46.0%, respectively compared to Gu et al. model, and by 68.5%, 30.3%, and 43.2%, respectively compared to Paulay and Priestly model.

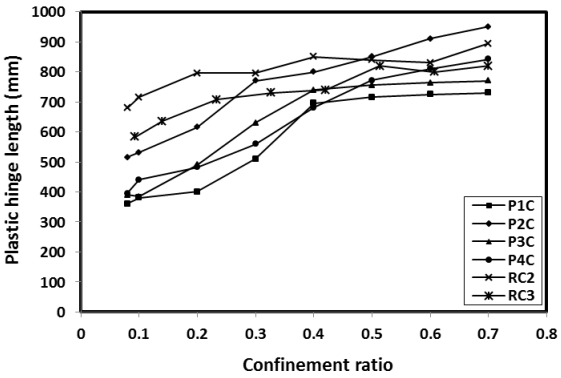

Figure 2. Effect of confinement ratio on the plastic hinge length

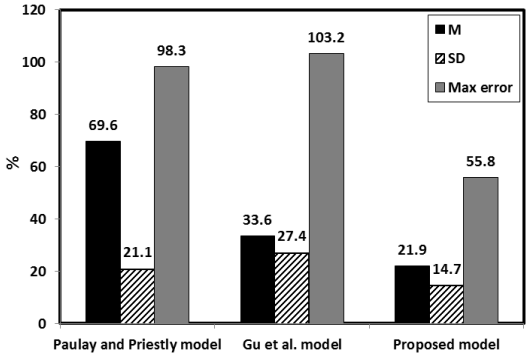

Figure 3. M, SD, and max error comparisons for all δ_u models.

7 CONCLUSIONS

The main findings of this study are summarized in the following points; 1) increasing the confinement ratio increases the plastic hinge length. 2) The proposed l_p model resulted in M and SD of 23.6% and 16.9%, respectively, compared to M and SD of 44.5% and 16.6%, respectively, in the Paulay and Priestley model predictions. 3) The proposed δ_u model decreased M, SD, and max. error by 34.8%, 46.3%, and 46.0%, respectively compared to Gu et al. δ_u model, and by 68.5%, 30.3%, and 43.2%, respectively compared to Paulay and Priestly δ_u model.

8 REFERENCES

ACI-318, 2011. Building Code Requirements for Structural Concrete and Commentary. American Concrete Institute.

ACI-440, 2008. Guide for the design and construction of externally bonded FRP systems for strengthening concrete structures. Reported by ACI Committee, 440

Binici, B., 2008. Design of FRPs in circular bridge column retrofits for ductility enhancement. Engineering Structures, 30:766-776

Desprez, C., Mazars, J., Kotronis, P. and Paultre, P., 2013. Damage model for FRP-confined concrete columns under cyclic loading. Engineering Structures, 48:519-531

Elsanadedy, H.M., Al-Salloum, Y.A., Alsayed, S.H. and Iqbal, R.A., 2012. Experimental and numerical investigation of size effects in FRP-wrapped concrete columns. Construction and Building Materials, 29:56-72

Elsanadedy, H.M. and Haroun, M.A., 2005. Seismic design guidelines for squat composite-jacketed circular and rectangular reinforced concrete bridge columns. ACI structural journal, 102

Gu, D.-S., Wu, G., Wu, Z.-S. and Wu, Y.-F., 2010. Confinement effectiveness of FRP in retrofitting circular concrete columns under simulated seismic load. Journal of Composites for Construction, 14:531-540

Gu, D.-S., Wu, Y.-F., Wu, G. and Wu, Z.-S., 2012. Plastic hinge analysis of FRP confined circular concrete columns. Construction and Building Materials, 27:223-233

Idris, Y. and Ozbakkaloglu, T., 2013. Seismic behavior of high-strength concrete-filled FRP tube columns. Journal of Composites for Construction, 17

Li, Y.-F. and Sung, Y.-Y., 2004. A study on the shear-failure of circular sectioned bridge column retrofitted by using CFRP jacketing. Journal of reinforced plastics and composites, 23:811-830

Ls-Dyna Keyword User's Manual, 2007. Version 971. Livermore Software Technology Corp., Livermore, CA, USA.

Malvar, L., Crawford, J. and Morrill, K., 2000. K&C concrete material model Release III–Automated generation of material model input. Karagozian and Case Structural Engineers, Technical Report TR-99-24.3.

Malvar, L., Crawford, J., Wesevich, J. and Simons, D., 1996. A new concrete material model for DYNA3D-Release II: shear dilation and directional rate enhancements. A Report to Defense Nuclear Agency under Contract No. DNA001-91-C-0059.

Mohammed, T.A., 2012. Reinforced concrete structural members under impact loading. PhD thesis, THE UNIVERSITY OF TOLEDO.

Ozbakkaloglu, T. and Idris, Y., 2014. Seismic Behavior of FRP-High-Strength Concrete–Steel Double-Skin Tubular Columns. Journal of Structural Engineering, 140

Ozbakkaloglu, T. and Saatcioglu, M., 2006. Seismic behavior of high-strength concrete columns confined by fiber-reinforced polymer tubes. Journal of Composites for Construction, 10:538-549

Ozbakkaloglu, T. and Saatcioglu, M., 2007. Seismic performance of square high-strength concrete columns in FRP stay-in-place formwork. Journal of Structural Engineering, 133:44-56

Paulay, T. and Priestly, M.J.N., 1992. Seismic Design of Reinforced Concrete and Masonry Buildings, New York, John Wiley & Sons, Inc.

Priestley, M., Seible, F. and Calvi, G., 1996. Seismic design and retrofit of bridges.

Sheikh, S.A. and Yau, G., 2002. Seismic behavior of concrete columns confined with steel and fiber-reinforced polymers. ACI structural journal, 99

Simons, D., 1995. Recent modifications to DYNA3D model 16 for concrete. Proceedings, DNACWE Structural Analysis Meeting, Logicon RDA, Albuquerque, NM:141-157

Wang, Z., Wang, D., Sheikh, S. and Liu, J., 2011. Seismic Performance of FRP-Confined Circular RC Columns. Advances in FRP Composites in Civil Engineering. Springer.

Xiao, Y., Wu, H. and Martin, G., 1999. Prefabricated composite jacketing of RC columns for enhanced shear strength. Journal of Structural Engineering, 125:255-264

Yazici, V. and Hadi, M.N., 2012. Normalized confinement stiffness approach for modeling FRP-confined concrete. Journal of Composites for Construction, 16:520-528

Youssf, O., Elgawady, M.A. and Mills, J.E., 2015. Experimental Investigation of FRP-confined Crumb Rubber Concrete Columns under Seismic Loading. In press,

Youssf, O., Elgawady, M.A., Mills, J.E. and Ma, X., 2014. Finite element modelling and dilation of FRP-confined concrete columns. Engineering Structures, 79:70-85

Zhao, X.-M., Wu, Y.-F. and Leung, A., 2012. Analyses of plastic hinge regions in reinforced concrete beams under monotonic loading. Engineering Structures, 34:466-482

Zhou, C., Lu, X., Li, H. and Tian, T., 2013. Experimental study on seismic behavior of circular RC columns strengthened with pre-stressed FRP strips. Earthquake Engineering and Engineering Vibration, 12:625-642